frontiers | Frontiers in Materials

TYPE Original Research
PUBLISHED 15 September 2023
DOI 10.3389/fmats.2023.1253747

OPEN ACCESS

EDITED BY
Han-Min Wang,
Tianjin University of Science and Technology, China

REVIEWED BY
Weiwei Zhang,
Beijing Technology and Business University, China
Ning Zhang,
Nanjing University of Science and Technology, China

*CORRESPONDENCE
Wenbin Guo,
wenbingwb2000@sina.com

†These authors have contributed equally to this work and share first authorship

RECEIVED 06 July 2023
ACCEPTED 06 September 2023
PUBLISHED 15 September 2023

CITATION
Guo W, Jiang X, De X, Zhai S, Shi T, Yang J, Zhang X and Wang Z (2023), Establishment and parameter analysis of the elasto-visco-plastic constitutive model for straw-potato residue mixture. *Front. Mater.* 10:1253747. doi: 10.3389/fmats.2023.1253747

Establishment and parameter analysis of the elasto-visco-plastic constitutive model for straw-potato residue mixture

Wenbin Guo*†, Xinyang Jiang†, Xuehong De†, Shuo Zhai, Tianyu Shi, Jian Yang, Xuhui Zhang and Zhipeng Wang

College of Mechanical and Electrical Engineering, Inner Mongolia Agricultural University, Hohhot, China

In an attempt to characterize the non-linear augmentation of stress as a function of strain during the compression molding process of the straw-potato residue mixture, and to analyze the impact of elasto-visco-plastic deformation on energy consumption and product quality, the present study has established an elasto-visco-plastic constitutive model for the straw-potato residue mixture based on stress-strain test data. The model parameters were obtained through curve fitting, including the elastic modulus *E*, viscous coefficient *K*, viscous index *n*, friction stress σ_f, and plastic coefficient $R^{1/m}$. The effects of test factors such as moisture content, feeding amount, compression temperature, and compression speed on these model parameters were analyzed to decipher the elasto-visco-plastic deformation process of the mixture. Additionally, specific energy consumption (*SEC*) and relaxation ratio (R_r) were employed as test indicators and were subjected to correlation analysis with the model parameters, culminating in the establishment of a multivariate regression equation. The results indicate that the correlation between *SEC* and the model parameters is quite significant under different test conditions, while R_r is significantly correlated with *n*, σ_f, and $R^{1/m}$ only under different moisture contents. This suggests that the energy consumption in the molding of the straw-potato residue mixture is primarily due to overcoming the resistance of elasto-visco-plastic deformation and friction, while the quality of the molding is mainly influenced by the moisture content, thereby establishing a connection with the elasto-visco-plastic parameters. The multivariate regression equation ultimately derived can be used to discern the degree of influence of elastic deformation, viscous deformation and plastic deformation on the specific energy consumption during the compression of the straw-potato residue mixture.

KEYWORDS

corn straw, potato residue, elasto-visco-plastic, constitutive model, correlation analysis

1 Introduction

Corn straw and potato residue represent significant biomass resources (Guo et al., 2021), characterized by their loose nature, low bulk density, and good compressibility. Consequently, they can be mixed and compacted into biomass pellets or briquetting (Guo et al., 2021), leveraging the excellent adhesive properties of potato residue to reduce energy consumption during molding and improve product quality. To achieve these objectives and optimize the molding process parameters, one can construct a

FIGURE 1
The Straw-potato residue mixture.

constitutive model of the straw-potato residue mixture compression to describe its elasto-visco-plastic deformation process.

Loose materials such as straw and potato residue exhibit pronounced elasto-visco-plastic deformation during compression, with the resultant stress nonlinearly escalating in response to increasing strain (Du et al., 2020; Guo et al., 2022). This escalation rate increases gradually as the strain increases. Initially, the material's packing state changes under external forces and the internal void ratio decreases, this results in a relatively slow increase in stress with strain, at this point, deformation is primarily elastic. Upon compression to a certain density, the material particles undergo viscous flow and plastic deformation. The inherent latency of visco-plastic deformation causes an abrupt acceleration in the stress increase rate with strain (Guo et al., 2022), exacerbating the wear and energy consumption of the compression equipment. Duo to the abrupt increase in stress during the compression process and the evident nonlinearity of the material stress-strain curve, traditional stress-strain models and rheological models do not adequately describe the nonlinear rise of stress with increasing strain. Consequently, the stress-strain curve during compression is frequently partitioned into pre-compression and molding phases (Huo et al., 2013; Li et al., 2020), and constitutive models have been established separately (Kaliyan et al., 2009a; Zhang, 2009) to analyze the material's elastic, viscous and plastic deformation.

In order to comprehensively decipher the stress-strain curve of loose agricultural materials, particularly the straw-potato residue mixture, and to obtain the elasto-visco-plastic characteristic parameters during compression, this study aims to construct an elasto-visco-plastic constitutive model for the straw-potato residue mixture through stress-strain test analysis. This model will elucidate the entire elasto-visco-plastic deformation process during compression, and the effects of elasto-visco-plastic deformation on the molding energy consumption and the quality of the molded product will be obtained through the analysis of the correlation between the model parameters and the test factors, energy consumption.

2 Materials and methods

2.1 Materials and device

The corn straw harvested naturally in autumn in Hohhot, Inner Mongolia, was used for test. The straw was crushed and sieved with a perforated screen to a particle size below 2 mm, with a moisture content of (4 ± 0.1) %. The potato residue, provided by a starch processing enterprise in Hohhot, Inner Mongolia, was used with a moisture content of (65% ± 1%) after mechanical dehydration. Before the experiment, the straw and potato residue were mixed in a mass ratio using an LJ-9818 multifunctional mixer, and the moisture content was measured, the sample of the straw-potato residue mixture is shown in Figure 1.

The mixture was weighed and stored in a refrigerated environment at 2–4°C to prevent material spoilage and reduce water loss. Compression tests were completed within a week. The test device included a DDL200 microcomputer-controlled electro-hydraulic servo universal testing machine and a self-made detachable compression device, as shown in Figure 2. During the test, the prepared straw-potato residue mixture was introduced into the compression device. An EDC digital controller, operated by a computer program, governs the plunger to execute axial compression. Upon completion of the test, the movable base plate is actuated, allowing the briquetting to descend through the discharge opening, thereby concluding the material drop process.

2.2 Method

During the compression of the straw-potato residue mixture, pronounced stress relaxation and creep phenomena are manifested (Guo et al., 2021; Wang, 2022). The resultant rheological parameters are frequently influenced by factors such as moisture content, feeding amount, and temperature. Therefore, this study the test factors and levels are selected as shown in Table 1. The moisture content of the mixture is determined by adjusting the mass ratio of straw fragments to potato residues. Each experiment is repeated three times, and the results are averaged.

2.2.1 Test indicators

To analyze the connection between the elasto-visco-plastic parameters of the straw-potato residue mixture and the energy consumption ratio, as well as the molding effect, the specific energy consumption (*SEC*) and the relaxation ratio (R_r) are utilized as test indicators. *SEC* represents the energy required to compress and mold a unit mass of the mixture, which can be derived from the force-displacement curve obtained from compressing the

10.3389/fmats.2023.1253747

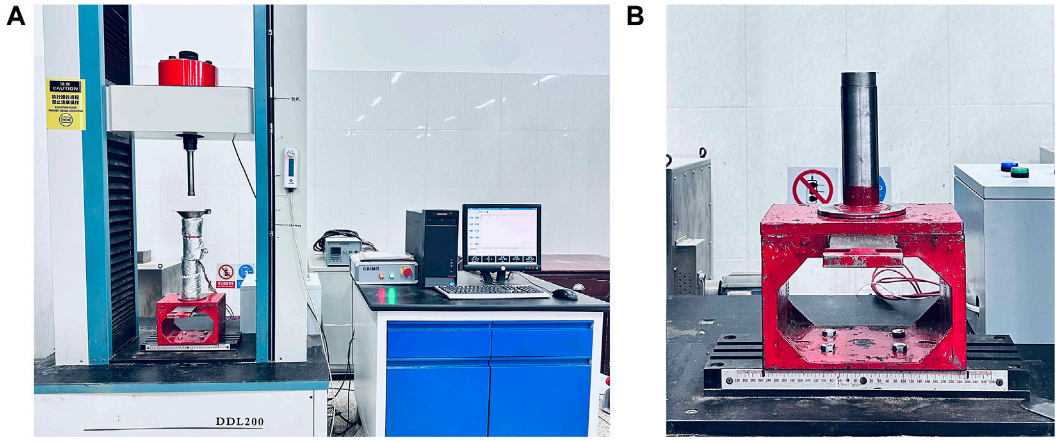

FIGURE 2
Test device. **(A)** Universal tester; **(B)** compression device.

TABLE 1 Test factors and levels.

Level	Moisture content/%	Feeding amount/g	Compression temperature/°C	Compression speed/mm·min^{-1}
1	35	20	20	10
2	44	25	50	40
3	49	30	80	70
4	52	35	110	100
5	55	40	140	130

straw-potato residue mixture (Li et al., 2018), as shown in Eq. 1. R_r is the ratio of the compressed density ρ of the straw-potato residue mixture to the relaxed density ρ_s of the block 24 h after demolding (Cui et al., 2020; Wang, 2022), as shown in Eq. 2.

$$SEC = \frac{W}{m} = \int \frac{F(s)}{m} ds \tag{1}$$

where SEC is the specific energy consumption (kJ/kg), W is the total energy consumption during the compression process (kJ), m is the mass of the mixture (kg), s is the displacement (mm), F is the loading force (kN).

$$R_r = \frac{\rho}{\rho_s} = \frac{\rho}{4m/\pi d^2 h} \tag{2}$$

where R_r is the relaxation ratio, ρ is the compression density (kg·m^{-3}), and ρ_s is the relaxation density (kg·m^{-3}), m is the mass of the briquetting (kg), d is the diameter of the briquetting (m), h is the height of the briquetting (m).

2.2.2 Constitutive models

According to the stress-strain curve characteristics of the straw-potato residue mixture, it can be deduced that the demarcation between elastic deformation, viscous deformation, and plastic deformation during the compression process is not distinctly discernible. Therefore, an elasto-visco-plastic constitutive model can be used to describe the stress-strain process of the straw-potato residue mixture. The mechanical analog model of this process, constituted by the parallel combination of a non-linear spring element, a damper viscous element, and a Coulomb friction element (Li et al., 2019), is demonstrated in Figure 3. The nonlinear spring element, which is utilized to describe the elasto-plastic deformation with the stress-strain relationship (Peleg, 1983; Nielsen et al., 2019), was modelled as:

$$\sigma_1(\varepsilon) = E\varepsilon + R\varepsilon^m \tag{3}$$

where $\sigma_1(\varepsilon)$ is the stress in the non-linear spring element, E is the elastic modulus, ε is the strain, R is the strength coefficient, m is the strain hardening exponent.

The damper viscous element, which is utilized to describe the viscous deformation, with the stress-strain relationship was modelled as (Huo et al., 2013):

$$\sigma_2(\varepsilon) = Ke^{n\varepsilon} \tag{4}$$

where $\sigma_2(\varepsilon)$ is the stress in the damper viscous element, ε is the strain, K is the viscous coefficient, n is the viscous index.

The Coulomb friction element, which is utilized to describe the frictional loss stress, with the stress-strain relationship was modelled as (Faborode and O'Callaghan, 1989; Ma et al., 2015):

$$\sigma_3(\varepsilon) = \sigma_f \tag{5}$$

where $\sigma_3(\varepsilon)$ is the stress in the Coulomb friction element, σ_f is the frictional loss stress.

10.3389/fmats.2023.1253747

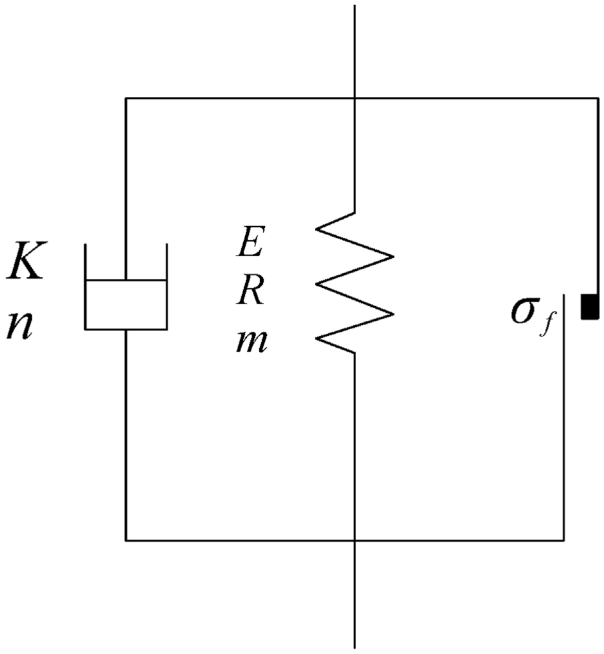

FIGURE 3
Elasto-visco-plastic mechanical analog model.

The total stress $\sigma(\varepsilon)$ in the elasto-visco-plastic constitutive model is the sum of the stress in the non-linear spring element $\sigma_1(\varepsilon)$, the damper viscous element $\sigma_2(\varepsilon)$ and the Coulomb friction element $\sigma_3(\varepsilon)$:

$$\sigma(\varepsilon) = E\varepsilon + R\varepsilon^m + Ke^{n\varepsilon} + \sigma_f \tag{6}$$

2.2.3 Curve fitting and parameter analysis

The elasto-visco-plastic constitutive model (Eq. 6) is used to fit the compression stress-strain curve of the mixture is fitted, and the resulting fit is shown in Figure 4. The results show that under different test factors and levels, the derived constitutive models exhibit high precision in fitting the stress-strain curve of the straw-potato mixture, with a coefficient of determination R^2 > 0.99. This indicates the applicability of the model in the study of the compressive properties of the mixture.

Through curve fitting and regression analysis, the model parameters of the elasto-visco-plastic constitutive model (Eq. 6) can be obtained, as shown in Table 2. To provide a more explicit analysis of the mixture's irreversible deformation throughout the compression process, the plastic coefficient $R^{1/m}$ is introduced (Koval'chenko, 1990), which is expressed as follows:

$$\sigma_s^{1/m} = R^{1/m}\varepsilon_s \tag{7}$$

where σ_s is the plastic stress, ε_s is the plastic strain, $R^{1/m}$ is the plastic coefficient. A larger value of $R^{1/m}$ indicates that a greater stress is required to produce the same plastic strain.

As shown in Table 2, under different moisture contents, the elastic modulus E and the frictional loss stress σ_f exhibit discernible variations. The higher moisture content during compression leads to decreased values of both E and σ_f, whereas the viscous index n increases. This results in the smaller stress generated by elastic deformation of the mixture, the higher stress generated by viscous deformation, and the smaller the frictional resistance during the compression process. As the moisture content of the material increases, the plastic coefficient $R^{1/m}$ also decreases. However, when the moisture content is above 44%, $R^{1/m}$ no longer decreases significantly and tends to stabilize. These results indicate that excessive moisture content is not conducive to plastic deformation of the mixture and that the viscous flow under pressure consumes the main stress.

Under different feeding amounts, E increases with the increase in feeding amount, while n and the strain hardening exponent m decrease, leading to an increase in $R^{1/m}$ with increasing feeding amount. This result indicates that when compressed to the same load, an increase in feeding amount will increase the stress generated by the elastic deformation of the mixture during compression, reduce the stress of viscous deformation, thereby reducing m, increasing $R^{1/m}$, and reducing the plastic deformation produced.

Under different compression temperatures, E, n, and σ_f generally increase with temperature, indicating that the higher the temperature, the greater the resistance to elasto-visco-plastic during the compression molding process. However, $R^{1/m}$ significantly decreases with increasing temperature, indicating that increasing the temperature can enhance the degree of plastic deformation of the mixture, thereby increasing the resistance to elasto-visco-plastic.

Under different compression speeds, the elasto-visco-plastic resistance of the straw-potato mixture responds differently to strain, so the higher the compression speed, the larger the E, n, and σ_f, but the degree of plastic deformation is less affected, and when the compression speed increases to more than 40 mm·min^{-1}, the size of $R^{1/m}$ tends to be constant.

3 Results and discussion

3.1 Curve analysis

The stress-strain curve obtained from the compression test of the straw-potato residue mixture is shown in Figure 5. During the compression process, stress gradually increases with the strain, initially at a slow rate, followed by a sharp acceleration. To better describe the stress-strain curve, it is divided into two stages: pre-compression and dense molding (Huo et al., 2013). During the pre-compression stage, the material is in a loose state at the beginning of compression. As the plunger contacts and squeezes, the air and water between the material particles are gradually squeezed out, and the gaps between the particles are gradually filled. Therefore, the deformation at this stage mainly comes from the elastic deformation and viscous flow of straw and potato residues. Upon entering the dense molding stage, as the plunger displacement continues to increase, the material particles begin to interlock with each other to form a denser structure, and the material mainly undergoes plastic deformation.

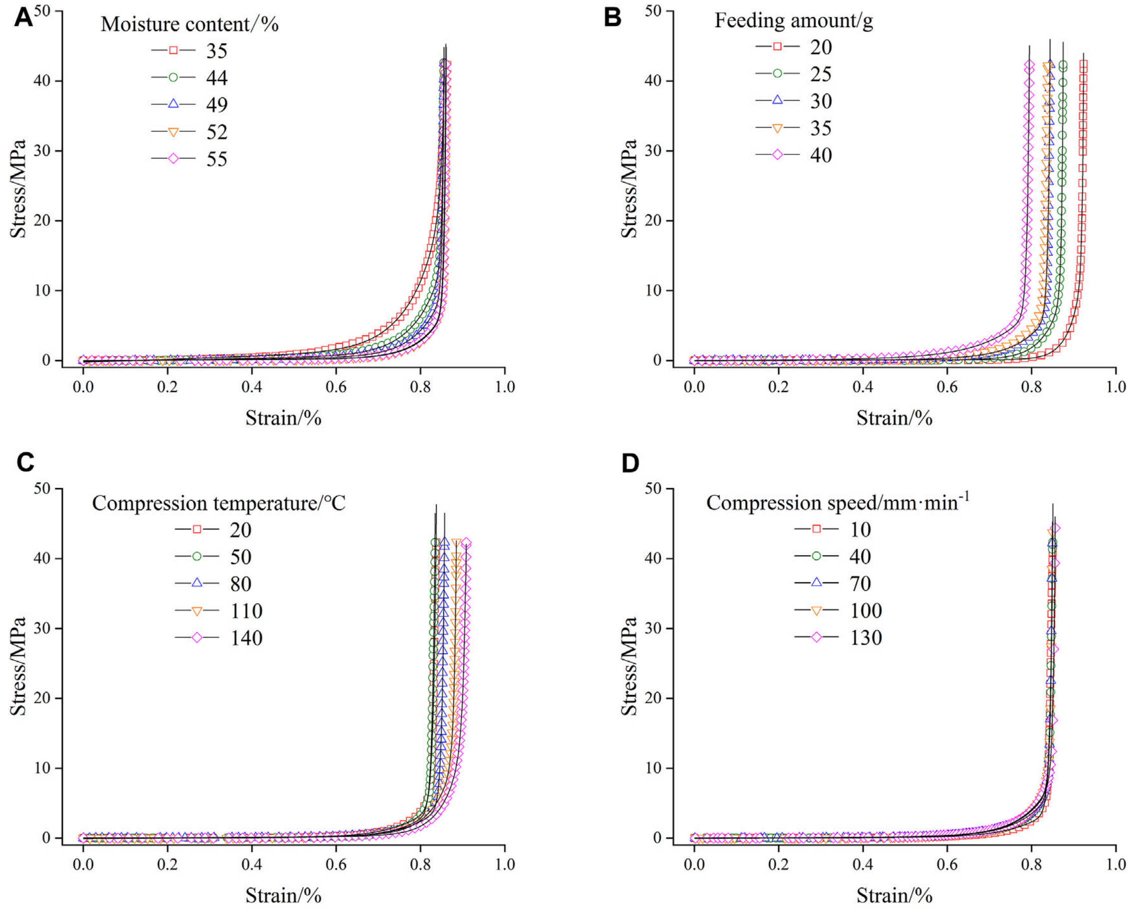

FIGURE 4
The compressive stress-strain curves of straw-potato residue mixture at different test factors and levels. **(A)** Different moisture contents; **(B)** Different feeding amounts; **(C)** Different compression temperatures; **(D)** Different compression speeds.

3.2 Effects of the test factors on the model parameters

To further encapsulate the influence of different test factors on the elasto-visco-plastic constitutive model (Eq. 6) parameters, a correlation analysis was conducted between the moisture content, feeding amount, compression temperature, compression speed, and the constitutive model parameters. The results are presented in Table 3. It is evident that E and n have significant correlations with all the test factors. Among them, the moisture content is extremely significantly negatively correlated with E and σ_f, and extremely significantly positively correlated with n; that is, the higher the moisture content, the smaller the elastic resistance and frictional resistance during the compression process of the mixture, and the higher the viscous resistance. $R^{1/m}$ is extremely significantly negatively correlated with moisture content and compression temperature, and extremely significantly positively correlated with feeding amount. This suggests that the higher the moisture content and temperature of the mixture, the smaller the $R^{1/m}$, and the more prone to produce plastic deformation. Conversely, the lower the feeding amount, the larger the $R^{1/m}$, making it less prone for the material to undergo plastic deformation during the compression process.

Multivariate regression analysis was conducted on E, n, σ_f, and $R^{1/m}$, including moisture content (Mc), feeding amount (Fa), compression temperature (Ct), and compression speed (Cs) as influencing factors. The obtained regression model and the results of the F-test are presented in Table 4. It is can be seen that although the influence weights of the test factors on the model parameters E, n, σ_f, and $R^{1/m}$ are different, the significance probability $p < 0.01$ in all cases, and the F-values are all greater than $F_{0.01}(4,15)$. Therefore, the multivariate regression equation obtained is extremely significant and can be used to describe the degree of association between the test factors and each model parameter, thereby clarifying the physical implications represented by the model parameters. Based on the results in Table 4, the standardized partial regression coefficients H_{Mc}, H_{Fa}, H_{Ct}, and H_{Cs} were calculated as shown in Table 5 (Yang, 2006). The magnitude of these coefficients reflects the influence weights of the test factors on the constitutive model parameters. Thus, the influence weights of the test factors on E, n, σ_f, and $R^{1/m}$ are ranked as follows:

10.3389/fmats.2023.1253747

TABLE 2 Elasto-visco-plastic model parameters of mixture at different test factors and levels.

Factors	Level	Elastic modulus E/MPa	Viscous coefficient K/MPa·s	Viscous index n	Strength coefficient R/MPa	Strain hardening exponent m	Frictional loss stress $\lvert\sigma_f\rvert$/MPa	Plastic coefficient $R^{1/m}$	R^2
Moisture content (%)	35	2.5077	1.4789E-4	13.8996	3.4585E+08	108.6286	0.2628	1.1984	0.9986
	44	1.0269	2.5717E-5	15.3931	5.3248E+15	210.4242	0.1451	1.1878	0.9989
	49	0.6527	9.0220E-6	16.2117	5.3579E+17	239.8370	0.0996	1.1856	0.9986
	52	0.3291	2.6637E-6	17.2179	2.2324E+15	212.7550	0.0407	1.1807	0.9972
	55	0.3331	4.3132E-6	16.6742	2.2101E+15	210.8648	0.0474	1.1824	0.9969
Feeding amount (g)	20	0.1734	7.5738E-13	33.0499	2.2235E+11	285.5870	0.0390	1.0958	0.9989
	25	0.1550	1.5337E-8	23.1844	4.4521E+15	243.2245	0.0264	1.1597	0.9975
	30	0.2361	4.2736E-5	14.1679	2.6237E+14	174.4243	0.0316	1.2097	0.9964
	35	0.2795	2.2730E-4	12.2652	1.6898E+13	152.6912	0.0337	1.2208	0.9962
	40	0.3943	2.0700E-3	10.1651	1.6971E+16	147.1280	0.0363	1.2892	0.9970
Compression temperature (°C)	20	0.0268	1.6154E-4	12.3648	3.3686E+11	128.6399	0.0011	1.2354	0.9917
	50	0.0485	3.8502E-5	13.9290	1.3579E+12	134.0820	0.0029	1.2317	0.9931
	80	0.1267	5.0573E-5	13.3899	2.7471E+11	146.9269	0.0048	1.1963	0.9935
	110	0.5088	2.8374E-7	19.8350	1.1995E+10	162.5153	0.0890	1.1530	0.9994
	140	0.4672	3.0351E-8	22.0766	1.1198E+07	135.1823	0.0944	1.1275	0.9994
Compression speed (mm·min^{-1})	10	0.0268	1.6154E-4	12.3648	3.3686E+11	128.6399	0.0011	1.2354	0.9917
	40	0.2319	4.9043E-5	13.9185	7.0093E+13	174.1655	0.0322	1.2009	0.9958
	70	0.3460	2.4759E-5	14.7610	1.1475E+15	190.6409	0.0509	1.1995	0.9969
	100	0.3714	1.6893E-5	15.3843	3.1785E+15	196.8375	0.0505	1.1988	0.9977
	130	0.4100	2.2943E-5	15.0284	1.1757E+14	185.2543	0.0581	1.1911	0.9972

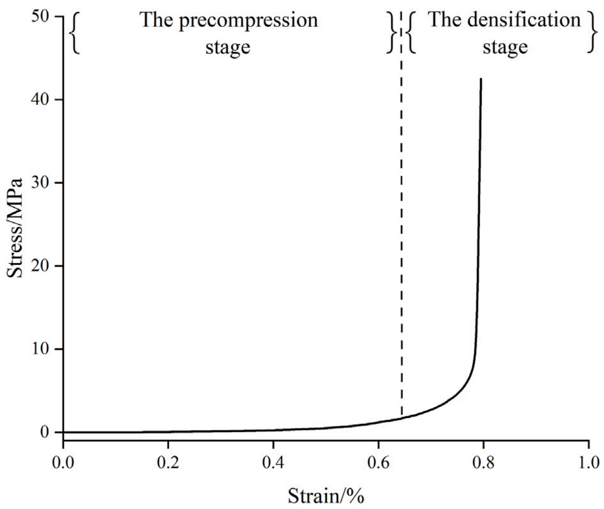

FIGURE 5
The stress-strain curve of the straw-potato residue mixture.

For E: Mc > Fa > Cs > Ct; for n: Fa > Ct > Mc > Cs; for σ_f: Mc > Ct > Cs > Fa; and for $R^{1/m}$: Fa > Ct > Cs > Mc. It is evident that the E and σ_f parameters of the material are primarily influenced by the moisture content; the lower the moisture content, the greater the elastic and frictional resistance during compression. $R^{1/m}$ and n are primarily influenced by the feeding amount; the higher the feeding amount, the smaller the n and the larger the $R^{1/m}$, making it less likely for plastic deformation to occur. Furthermore, the parameter $R^{1/m}$, which measures the material's capacity for plastic deformation, is significantly affected by temperature. The higher the moisture content, the smaller the $R^{1/m}$ value, and the greater the plastic strain produced by the straw-potato residue mixture under the same stress conditions.

3.3 Effects of the model parameters on the test indicators

Establishing a connection between the constitutive model parameters and test indicators such as specific energy consumption and relaxation ratio helps to analyze and verify the physical meanings of E, n, σ_f, and $R^{1/m}$. It helps clarify the influence of mechanical characteristic parameters during the compression process of the straw-potato residue mixture on the quality of the briquetting and energy consumption. Table 6 presents the correlation analysis results between specific energy consumption, relaxation ratio, and model parameters under different test factors. It is evident that under different test factors, model parameters significantly correlated with the specific energy consumption (*SEC*) emerge.

Regarding the relaxation ratio, which characterizes the quality of the briquetting, an extremely significant positive correlation with $R^{1/m}$ only appears under different moisture contents. This suggests that during the compression stage where stress increases with strain (the stress-strain stage), the higher the moisture content in the mixture, the smaller the $R^{1/m}$, and the lesser the force required for plastic deformation. However, the significant negative correlation between the relaxation ratio and n, σ_f (Table 6) implies that the higher the moisture content of the material, the lower the viscous resistance and frictional resistance during compression. Consequently, it fails to meet the requirements for plastic deformation, ultimately resulting in lower quality after the straw-potato residue mixture is granulated. Therefore, to improve the quality of the product, it is necessary to further reduce the moisture content or increase the viscous and frictional resistance.

Under different moisture contents, *SEC* is extremely significantly correlated with all model parameters. It exhibits an extremely significant negative correlation with n, and an extremely significant positive correlation with E, σ_f, and $R^{1/m}$. This indicates that under different moisture contents, the higher the elasto-visco-

TABLE 3 Correlation analysis between test factors and model parameters.

	E	K	n	$\lvert\sigma_f\rvert$	$R^{1/m}$
Moisture content	−0.9695** ($p < 0.01$)	−0.9161* ($p < 0.05$)	0.9597** ($p < 0.01$)	−0.9852** ($p < 0.01$)	−0.9639** ($p < 0.01$)
Feeding amount	0.9452* ($p < 0.05$)	0.7613 (0.1348)	−0.9438* ($p < 0.05$)	0.1401 (0.8222)	0.9807** ($p < 0.01$)
Compression temperature	0.9067* ($p < 0.05$)	−0.8625 (0.0599)	0.9222* ($p < 0.05$)	0.9170* ($p < 0.05$)	−0.9758** ($p < 0.01$)
Compression speed	0.9245* ($p < 0.05$)	−0.8146 (0.0931)	0.8861* ($p < 0.05$)	0.9086* ($p < 0.05$)	−0.8270 (0.0841)

Note: Asterisks (**) and (*) indicate that the correlation is significant at the 0.01 level and 0.05 level (p-values shown in parentheses).

TABLE 4 Multivariate regression equations of model parameters and test factors and F-test results.

Multivariate regression equation	F	p	R^2
$E = 6.2105 - 0.1261M_c + 0.0113F_a - 1.6475 \times 10^{-6}C_t - 2.2758 \times 10^{-5}C_s$	11.3893	< 0.0010	0.7523
$n = 42.0717 + 0.1529M_c - 1.1337F_a - 0.0310C_t - 0.0120C_s$	9.6457	0.0020	0.7200
$\sigma_f = 0.6916 - 0.0133M_c + 3.8000\times 10^{-5}F_a + 2.1076\times 10^{-4}C_t + 5.6103\times 10^{-5}C_s$	7.0905	< 0.0010	0.6540
$R^{1/m} = 0.9545 - 2.2749 \times 10^{-4}M_c + 0.0090F_a - 4.7360 \times 10^{-4}C_t - 6.5377 \times 10^{-5}C_s$	12.6924	< 0.0010	0.7719

Note: $F_{0.01}(4,15) = 4.893$, $F_{0.05}(4,15) = 3.06$.

TABLE 5 Standardized partial regression coefficients of model parameters and test factors.

Model parameter	Standardized partial regression coefficient			
	H_{Mc}	H_{Fd}	H_{Ct}	H_{Cs}
E	−0.8639	0.0759	0.0001	−0.0014
n	0.1110	−0.8054	0.2094	−0.0812
σ_f	−0.8096	0.0023	0.1193	0.0318
$R^{1/m}$	−0.0204	0.7874	−0.3949	−0.0545

plastic resistance during compression, the easier it becomes to form, and the smaller the $R^{1/m}$, the less stress required to produce the same plastic strain, resulting in lower specific energy consumption. Under different feeding amounts, *SEC* is extremely significantly positively correlated with E and significantly positively correlated with $R^{1/m}$. This suggests that the higher the feeding amount, the higher the elastic resistance during compression, leading to higher energy consumption. When compressed to the same load, the plastic strain produced is smaller, hence $R^{1/m}$ is greater. Under different temperatures, *SEC* is significantly positively correlated with n, σ_f, and significantly negatively correlated with $R^{1/m}$. This implies that influenced by temperature, the higher the material's viscous and frictional resistance during compression, the higher the energy consumption. When compressed to the same load, the plastic strain produced is greater and therefore $R^{1/m}$ is smaller. Under different compression speeds, *SEC* is only significantly positively correlated with E and σ_f. This is because when the compression speed is relatively fast, viscous deformation is delayed and does not occur in a timely manner. Therefore, influenced by the compression rate, energy consumption is mainly due to elastic deformation and friction, and the higher the elastic resistance and frictional resistance, the higher the energy consumption.

In accordance with the relationship between the test indicators and the model parameters, a multivariate regression analysis of the model parameters with specific energy consumption and relaxation ratio was conducted, thereby establishing a multivariate regression model as shown in Table 7. The results showed that the F-value of the specific energy consumption with model parameters exceeded $F_{0.01}(4,19)$, thus the multivariate regression equation of specific energy consumption with model parameters exhibited a highly significant linear relationship. Conversely, the F-value of the relaxation ratio with model parameters was less than $F_{0.05}(4,19)$, therefore the multivariate regression equation of the relaxation ratio with model parameters presented an insignificant linear relationship, and the resulting equation eliminated the $R^{1/m}$ term. From this, it is evident that the molding energy consumption of the straw-potato residue mixture primarily originates from the stress-strain stage, and its connection with the stress-strain model parameters is relatively tight. However, the quality indicators of briquetting are not closely associate with the stress-strain model parameters and are primarily influenced by the holding stage parameters such as holding time and pressure (Wang, 2022).

In accordance with the results presented in Table 7, the standardized partial regression coefficients were obtained as shown in Table 8. The significance of the impact of the stress-strain model parameters on the *SEC* is in the following order: $E > R^{1/m} > \sigma_f > n$. This indicates that elastic resistance, plastic deformation, and frictional resistance are the primary contributors to energy consumption. The significance of the impact of the stress-strain model parameters on the R_r is as follows: $E > \sigma_f > n$. This suggests that although the quality of the briquetting is influenced by the elastic resistance and frictional resistance during the stress-strain stage, the degree of this influence is limited.

TABLE 6 Correlation analysis between test indicators and model parameters.

		E	K	n	$\lvert\sigma_f\rvert$	$R^{1/m}$
Moisture content	*SEC*	0.9967** ($p < 0.01$)	0.9847** ($p < 0.01$)	−0.9617** ($p < 0.01$)	0.9775** ($p < 0.01$)	0.9815** ($p < 0.01$)
	R_r	0.8669 (0.0571)	0.7827 (0.1175)	−0.8897* ($p < 0.05$)	−0.9086* ($p < 0.05$)	0.9870** ($p < 0.01$)
Feeding amount	*SEC*	0.9860** ($p < 0.01$)	0.8548 (0.0650)	−0.8063 (0.0993)	0.3501 (0.5635)	0.8987* ($p < 0.05$)
	R_r	−0.3432 (0.5717)	−0.2506 (0.6843)	0.7785 (0.1209)	0.7345 (0.1575)	−0.7042 (0.1843)
Compression temperature	*SEC*	0.8670 (0.0570)	−0.5793 (0.3061)	0.9485* ($p < 0.05$)	0.9202* ($p < 0.05$)	−0.9253* ($p < 0.05$)
	R_r	−0.6674 (0.2184)	0.3810 (0.5269)	−0.8277 (0.0836)	−0.7816 (0.1184)	0.6809 (0.2057)
Compression speed	*SEC*	0.9012* ($p < 0.05$)	−0.7712 (0.1268)	0.8251 (0.0855)	0.8975* ($p < 0.05$)	−0.8271 (0.0841)
	R_r	0.3965 (0.5088)	−0.6233 (0.2613)	0.4676 (0.4272)	0.4041 (0.4998)	−0.5543 (0.3323)

TABLE 7 Multivariate regression equations of test indicators and model parameters and F-test results.

Multivariate regression equation	F	p	R^2
$SEC = -2.6166 + 2.4206E - 0.0092n + 2.5566\sigma_f + 4.1156R^{1/m}$	35.5980	< 0.0010	0.9047
$R_r = 1.8710 + 0.6497E + 0.0138n - 5.4261\sigma_f$	2.9863	0.0620	0.3590

TABLE 8 Standardized partial regression coefficients of test indicators and model parameters.

Test indicator	Standardized partial regression coefficient			
	H_E	H_n	$H_{\sigma f}$	$H_{R1/m}$
SEC	0.8495	−0.0305	0.1008	0.1102
R_r	2.7102	0.5418	−2.5435	

4 Conclusion and discussion

In this paper, an elasto-visco-plastic constitutive model for straw-potato residue mixture has been established, the model parameters that characterize the elasto-visco-plastic of the materials have been obtained, the correlations between the model parameters and the test factors and test indicators have been analyzed, and the influences of the test factors on the model parameters as well as the influences of the model parameters on the test indicators have been obtained through multivariate regression analyzes. The results show that: 1) The established elasto-visco-plastic constitutive model of the straw-potato residue mixture can accurately describe the nonlinear growth rule of the stress with the increase of strain during compression. 2) According to the correlation analysis, it is found that the elastic modulus E and the viscous coefficient n have significant correlation with all the test factors, the plastic parameter $R^{1/m}$ is extremely significantly correlation with moisture content, temperature, and feeding amount; there is a significant correlation between the specific energy consumption and the model parameters, and the relaxation ratio is only significantly correlated with $R^{1/m}$, n and friction loss stress σ_f under different moisture contents, which indicates that except for moisture content, the quality of briquetting is not closely related to the mechanical parameters in the stress-strain stage. 3) By establishing a multivariate regression model, the degree of influence of each test factor on model parameters and the degree of influence of the model parameters on the test indicators were determined, in which E and σ_f were mainly influenced by moisture content, while $R^{1/m}$ and n were mainly influenced by feeding amount; the specific energy consumption and relaxation ratio were mainly influenced by E. Bai et al., 2009, Chen et al., 2010, Gao et al., 2018, Joyner et al., 2021, Kaliyan and Morey, 2009b, Kaliyan and Morey, 2010, Le et al., 2016, Liao et al., 2022, Liu et al., 2010, Zhang et al., 2015, Zheng et al., 2005.

Data availability statement

The original contributions presented in the study are included in the article/Supplementary Material, further inquiries can be directed to the corresponding author.

Author contributions

WG: Investigation, Methodology, Resources, Writing–original draft, Writing–review and editing. XJ: Investigation, Writing–review and editing, Data curation, Methodology. XD: Investigation, Methodology, Supervision, Writing–review and editing. SZ: Investigation, Writing–review and editing. TS: Investigation, Writing–review and editing. JY: Investigation, Writing–review and editing. XZ: Investigation, Writing–review and editing. ZW: Supervision, Writing–review and editing, Investigation.

Funding

The authors are grateful for the support of the Chinese National Natural Science Foundation (31960365, 51766016) and the National key R&D program of China (2016-YFD-0701704).

Conflict of interest

The authors declare that the research was conducted in the absence of any commercial or financial relationships that could be construed as a potential conflict of interest.

Publisher's note

References

Bai, W., Hu, J., Lei, Y., Shi, X., and Yang, Z. (2009). Experimental study on straw cold molding by pressure and its regression analysis. *Henan Sci.* 27 (6), 703–706. doi:10.3969/j.issn.1004-3918.2009.06.020

Chen, X., Lu, P., Dong, Y., and Jia, J. (2010). The research of surface crack of biomass briquetting's products. *J. Agric. Mech. Res.* 32 (2), 185–190. doi:10.13427/j.cnki.njyi.2010.02.006

Cui, X., Yang, J., Deng, L., Lei, W., Huang, T., and Bai, C. (2020). Effect of different parameters on energy consumption of biomass pellet in single pelletization. *Acta Energiae Solaris Sin.* 41 (2), 27–32. doi:10.19912/j.0254-0096.2020.02.005

Du, X., Mao, H., and Wang, C. (2020). Compression characteristics and the influencing factors of sweet sorghum straw: experimental study. *BioResources* 15 (4), 9429–9443. doi:10.15376/biores.15.4.9429-9443

Faborode, M. O., and O'Callaghan, J. R. (1989). A rheological model for the compaction of fibrous agricultural materials. *J. Agric. Eng. Res.* 42 (3), 165–178. doi:10.1016/0021-8634(89)90048-6

Gao, J., Guo, W., and Yu, Z. (2018). Study on the compressibility of potato residue. *Food & Mach.* 34 (2), 50–53. doi:10.13652/j.issn.1003-5788.2018.02.011

Guo, W., Hu, F., De, X., Hou, Z., Wang, Z., and Jiang, X. (2022). Description of the instantaneous stress drop behavior of a cornstraw-potato residue mixture based on stress relaxation models. *BioResources* 17 (3), 5255–5267. doi:10.15376/biores.17.3.5255-5267

Guo, W., Qi, W., Wang, Z., and Wang, C. (2021a). Analysis on the research status and development of agricultural and forestry waste resource utilization under the condition of blending and briquetting. *J. China Agric. Univ.* 26 (1), 143–150. doi:10.11841/j.issn.1007-4333.2021.01.15

Guo, W., Wang, Z., Hou, Z., Hu, F., Wang, C., and Qi, W. (2021b). Parameter analysis and development of fractional calculus model forstress relaxation of cornstalk and potato residues. *Trans. Chin. Soc. Agric. Eng.* 37 (13), 284–290. doi:10.11975/j.issn.1002-6819.2021.13.032

Huo, L., Zhang, L., Tian, Y., Yao, Z., and Meng, H. (2013). Viscoelastic constitutive model of biomass pellet. *Trans. Chin. Soc. Agric. Eng.* 29 (09), 200–206. doi:10.3969/j.issn.1002-6819.2013.09.026

Joyner, C., Fernando, C., and Jaime, J. G. (2021). Visco-elastic-plastic model to represent the compression behaviour of sugarcane agricultural residue. *Biosyst. Eng.* 212, 378–387. doi:10.1016/j.biosystemseng.2021.11.009

Kaliyan, N., and Morey, R. V. (2009a). Constitutive model for densification of corn stover and switchgrass. *Biosyst. Eng.* 104 (1), 47–63. doi:10.1016/j.biosystemseng.2009.05.006

Kaliyan, N., and Morey, R. V. (2009b). Factors affecting strength and durability of densified biomass products. *Biomass Bioenergy* 33 (3), 337–359. doi:10.1016/j.biombioe.2008.08.005

Kaliyan, N., and Morey, R. V. (2010). Natural binders and solid bridge type binding mechanisms in briquettes and pellets made from corn stover and switchgrass. *Bioresour. Technol.* 101 (3), 1082–1090. doi:10.1016/j.biortech.2009.08.064

Koval'chenko, M. S. (1991). A rheological model of pressing of powders. *Soviet Powder Metallurgy Metal Ceram.* 29 (9), 753–756. doi:10.1007/BF00795589

Le, X., An, J., Zhang, G., Wang, L., Fan, J., Wang, P., et al. (2016). Investigation of the structural characteristics of corn stalk during hot-pressing. *BioResources* 11 (4), 10213–10225. doi:10.15376/biores.11.4.10213-10225

Li, W., Jiang, Y., Rao, S., Yin, X., Jiang, E., Shen, Z. L., et al. (2018). Volumetric-based image guidance is superior to marker-based alignments for stereotactic body radiotherapy of prostate cancer. *Trans. Chin. Soc. Agric. Eng.* 34 (1), 198–203. doi:10.1002/acm2.12280

Li, Z., Yan, L., Gao, Y., Wang, H., and Wang, P. (2019). Research status on biomass compression molding process model. *Sci. Technol. Eng.* 19 (12), 1–7. doi:10.3969/j.issn.1671-1815.2019.12.001

Li, Z., Yan, L., Gao, Y., Wang, P., and De, X. (2020). Research on model for Salix psammophila granules in compression process. *Forg. Stamp. Technol.* 45 (1), 89–95. doi:10.13330/j.issn.1000-3940.2020.01.014

Liao, P., Chen, X., Lin, H., Wang, Q., and Hang, W. (2022). Research progress of rheology applied in solid agricultural materials processing. *J. Chin. Agric. Mech.* 43, 84–91. doi:10.13733/j.jcam.issn.2095-5553.2022.03.011

Liu, J., Bai, X., Li, X., and Li, J. (2010). Shading the whole vines during young fruit development decreases ascorbate accumulation in kiwi. *J. Agric. Mech. Res.* 32 (08), 225–237. doi:10.1111/j.1399-3054.2010.01395.x

Ma, Y., Zhang, J., and Wu, Y. (2015). *Agricultural materials science*. Beijing, China: Chemical Industry Press.

Nielsen, S. K., Rezaei, H., Mandø, M., and Sokhansanj, S. (2019). Constitutive modelling of compression and stress relaxation in pine pellets. *Biomass Bioenergy* 130, 105370. doi:10.1016/j.biombioe.2019.105370

Peleg, K. (1983). A rheological model of nonlinear viscoplastic solids. *J. Rheology* 27 (5), 411–431. doi:10.1122/1.549714

Wang, Z. (2022). *Experimental study on creep characteristics of Co-briquetting of corn straw and potato pulp*. Hohhot, China: Inner Mongolia Agricultural University.

Yang, X. (2006). *Study on rheological properties and damage control of hetao muskmelons during storage and transportation*. Hohhot, China: Inner Mongolia Agricultural University.

Zhang, X., Hou, M., Song, L., Zhu, L., and Liu, K. (2015). Research progress on the densification and formation of agricultural and forestry solid organic wastes. *J. Technol.* 15 (1), 67–73+85. doi:10.3969/j.issn.1671-7333.2015.01.012

Zhang, X. (2009). *Study on the compressibility of korshinsk peashrub and its StressRelaxation characteristics*. Hohhot, China: Inner Mongolia Agricultural University.

Zheng, X., Lin, G., Li, Z., and Wang, S. (2005). Nonlinear Viscous-elastic-plasticity constitutive model of rapeseed and rapeseed kernel. *Trans. Chin. Soc. Agric. Mach.* 11, 93–97+107. doi:10.3969/j.issn.1000-1298.2005.11.022

10.3389/fmats.2023.1253747

Nomenclature

SEC	Specific Energy Consumption
R_r	Relaxation ratio
E	Elastic modulus
R	Strengthening coefficient
m	Strain hardening index
K	Viscous coefficient
n	Viscous index
σ_f	Friction loss stress
$R^{1/m}$	Plastic coefficient
$\sigma_1(\varepsilon)$	Stress in the non-linear spring element
$\sigma_2(\varepsilon)$	Stress in the damper viscous element
$\sigma_3(\varepsilon)$	Stress in the Coulomb friction element
$\sigma(\varepsilon)$	Total stress
σ_s	Plastic stress
ε_s	Plastic strain
Mc	Moisture content
Fa	Feeding amount
Ct	Compression temperature
Cs	Compression speed
H_{Mc}	Standardized partial regression coefficient of moisture content
H_{Fa}	Standardized partial regression coefficient of feeding amount
H_{Ct}	Standardized partial regression coefficient of compression temperature
H_{Cs}	Standardized partial regression coefficient of compression speed